InGaN/GaN Quantum Well Growth on Pyramids of Epitaxial Lateral Overgrown GaN

X. ZHANG,[1] P.D. DAPKUS,[2] D.H. RICH,[1] I. KIM,[2] J.T. KOBAYASHI,[1] and N.P. KOBAYASHI[1]

1.—Compound Semiconductor Laboratory, Department of Materials Science and Engineering, University of Southern California, Los Angeles, CA 90089. 2.—Compound Semiconductor Laboratory, , Department of Electrical Engineering/Electrophysics, University of Southern California, Los Angeles, CA 90089

InGaN/GaN quantum wells (QW) were grown by metalorganic chemical vapor deposition (MOCVD) on pyramids of epitaxial lateral overgrown (ELO) GaN samples. The ELO GaN samples were grown by MOCVD on sapphire (0001) substrates that were patterned with a SiN_x mask. Scanning electron microscopy and cathodoluminescence (CL) imaging experiments were performed to examine lateral variations in structure and QW luminescence energy. CL wavelength imaging (CLWI) measurements show that the QW peaks on the top of the grooves are red-shifted in comparison with the QW emission from the side walls. The results show that In atoms have migrated to the top of the pyramids during the QW growth. The effects of V/III ratio, growth temperature as well as ELO GaN stripe orientation on the QW properties are also studied.

Key words: Epitaxial lateral overgrown (ELO), InGaN quantum well (QW), indium migration, cathodoluminescence

INTRODUCTION

The epitaxial lateral overgrowth (ELO) of GaN on sapphire,[1] SiC,[2] and Si(111)[3,4] has demonstrated marked reductions in the defect density in regions where the lateral epitaxy has occurred over the dielectric mask. This approach has enabled the fabrication of high quality GaN-based laser diodes with estimated lifetimes of longer than 10,000 h.[5] Depending on the growth conditions, the ELO GaN will exhibit either a rectangular or triangular cross-section.[1-3] The later case permits the growth of GaN with V-grooves and provides for the possibility to grow and fabricate regular arrays of low dimensional structures (i.e., quantum wires and dots) based on nitride materials.

In this paper, we present results of the growth of InGaN QWs on GaN pyramids which were, in turn, obtained by ELO of GaN on sapphire substrates. We show that the In incorporation, the composition of the InGaN QW, and In migration towards the top of the pyramids depend on the orientation of the starting ELO GaN stripes, QW growth temperatures, and the V/III ratio. Cathodoluminescence (CL) wavelength imaging (CLWI) and local CL spectroscopy were performed in order to evaluate spatial variations in the effective QW bandgap caused by lateral variations in the In composition of the QW. These CL results reveal a red-shift of ~28 nm in the QW emission on the top of the pyramids relative to emission from the side walls, strongly suggesting that the In atoms tend to migrate from GaN side-wall to the top during the growth and incorporation.

(Received June 29, 1999; accepted September 1, 1999)

EXPERIMENTAL PROCEDURE

GaN buffer layers were grown on c-plane sapphire substrates using a multi-buffer layer approach by atmospheric pressure MOCVD in a close spaced showerhead reactor.[6] Trimethylgallium (TMGa), Trimethylindium (TMIn) and NH_3 were used as precursors. A 170 nm-thick SiN_x mask was then deposited by plasma-enhanced chemical vapor deposition (PECVD) using SiH_4 and N_2 precursors. Conventional photolithography and reactive ion etching (RIE) were used to form patterned stripes, with a 4 μm wide opening and 10 μm spacing, oriented along either the GaN $[11\bar{2}0]$ or $[1\bar{1}00]$ directions. The ELO GaN was grown at 1000°C for ~ 1 h, resulting in stripes with triangular cross-sections. Subsequently, a 4-nm-thick InGaN QW was grown and capped with a 70 nm-thick

Table I. Sample Specifications

	A	B	C	D
Growth Temp.(°C)	750	750	750	775
V/III Ratio	2070	2070	1035	2070
Stripe Orientation	[11$\bar{2}$0]	[1$\bar{1}$00]	[11$\bar{2}$0]	[11$\bar{2}$0]

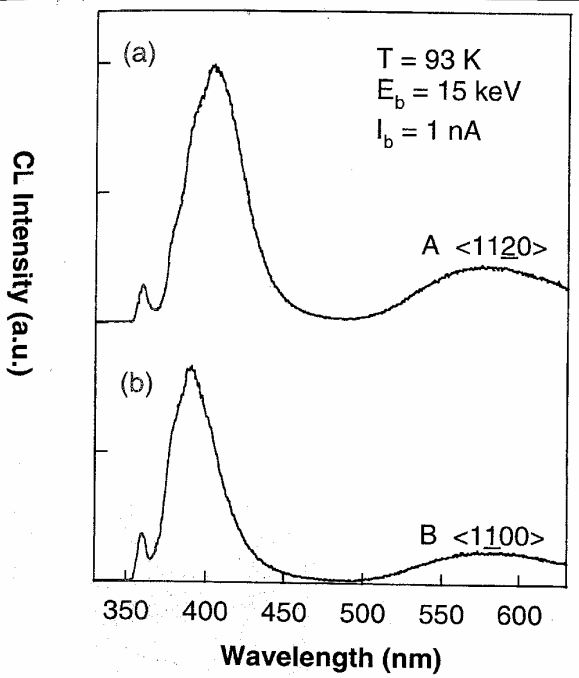

Fig. 1. Spatially averaged CL spectra for (a) samples A and (b) samples B.

GaN layer. The InGaN QWs are grown at either 740°C or 775°C. While lateral variations in the In composition are expected owing to the In migration along the pyramids facets, similar growth conditions were used to grow InGaN QWs with a ~15% In composition on unpatterned GaN substrates.

The CL experiments were performed with a modified JEOL-840A scanning electron microscope using a 15 keV e-beam. The temperature of the samples were maintained at 93 K. CLWI was performed by acquiring a series of discrete monochromatic images, constructing a local spectrum at all 640 × 480 scan points within the image, and determining the wavelength, $\lambda_m(x,y)$, at which there is a peak in the CL spectrum at each scan point (x,y). CLWI thus enables a spatial mapping of the effective band gap, which has been used to investigate the phase segregation of InGaN QWs grown on unpatterned substrates.[7] We have studied here four ELO samples (i.e., samples A–D), whose growth conditions and stripe direction are shown in Table I.

RESULTS AND DISCUSSION

Figure 1 shows spatially averaged CL spectra for samples A and B over a region of 64 μm × 49 μm area.

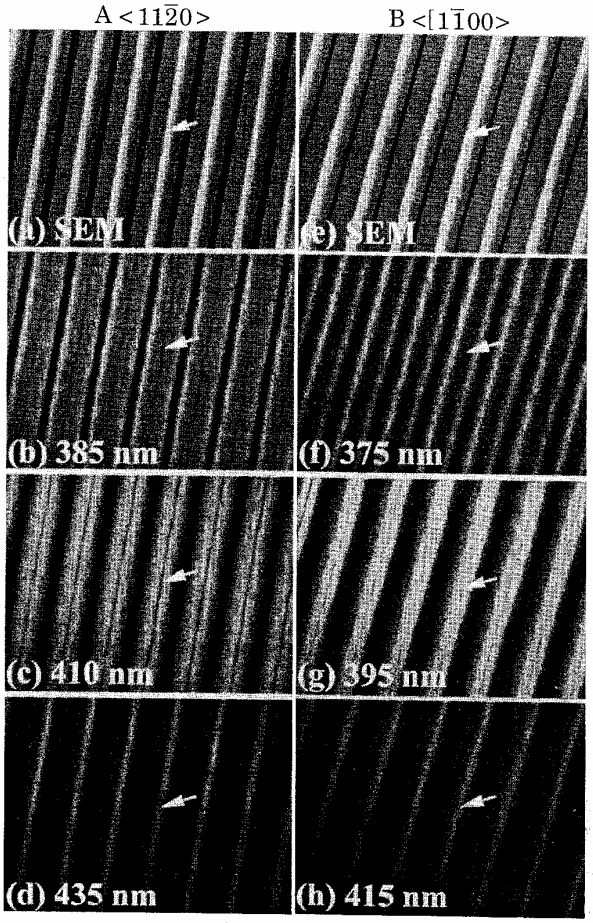

Fig. 2. SEM and CL images for samples A and B respectively. The arrows indicate the top of ELO GaN stripes.

SEM and CL images over the same regions for samples A and B are shown in the Fig. 2a–2d and Fig. 2e–2h, respectively. Sample A, with an ELO GaN stripe orientation along [11$\bar{2}$0], exhibits an InGaN QW peak emission that is red-shifted by ~15 nm in comparison to sample B, which possesses the [1$\bar{1}$00] ELO stripe orientation, as shown in the spectra of Fig. 1. These results indicate that In incorporation in the QW is enhanced when the ELO stripe is oriented along [11$\bar{2}$0] direction in comparison to the [1$\bar{1}$00] stripe orientation.

The arrows in Fig. 2a–2d and Fig. 2f–2h mark the same position on the top of ELO GaN stripes for each of the SEM and CL images for samples A and B. Figure 2b, c, and d are monochromatic CL images of sample A, acquired at 385 nm, 410 nm, and 435 nm, respectively. The 410 nm position represents the QW peak wavelength of the spatially averaged CL spectrum of sample A, as shown in Fig. 1a. The CL images of sample A in Fig. 2 show that the short wavelength emission is mostly from the lower pyramid edge, while the long wavelength emission is from the top. In Fig. 2c, the peak wavelength emission at 410 nm (sample A) originates from nearly all of the side wall

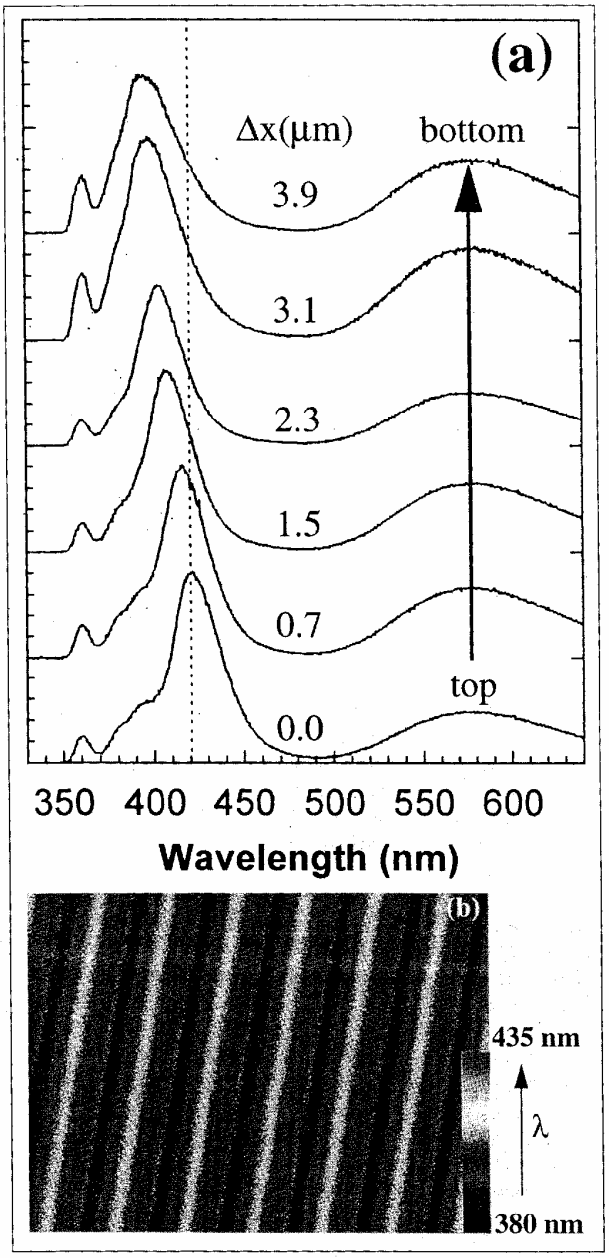

Fig. 3. (a) Local CL spectra, and (b) CLWI images of sample A.

of a stripe, in contrast with a notable absence of this emission from the top.

For sample B, the CL image (Fig. 2h at 415 nm) of the long wavelength emission is similar to the corresponding image for sample A in Fig. 2d. The long wavelength QW emission for both samples is localized near the pyramid tops. In contrast, the peak wavelength (395 nm) and short wavelength (375 nm) emissions of sample B show a greater degree of localization near the stripes edges and stripe tops, respectively, relative to the corresponding images (410 nm and 385 nm) of sample A in Fig. 2. Therefore, the stripe direction strongly influences the subsequent QW optical properties, both in wavelength and localization.

In order to further analyze the spatial variation of the QW energy across the ELO GaN stripe, local CL spectra as well as CLWI images of sample A were acquired, as shown in Fig. 3a and b, respectively. Local CL spectra are shown for various e-beam positions, Δx, relative to the top of the pyramid (i.e., where Δx = 0). A 28 nm blue shift of the QW peak wavelength is shown in Fig. 3a as the e-beam is moved from the top to the bottom of the GaN stripe.

CLWI images for sample A were obtained over the same area of sample A for which the monochromatic images of Fig. 2a were acquired. The mapping of λ_m into a color-scale representation is shown by the color-scale bar indicating the wavelength scale. The λ_m for sample A gradually increases from the edge to the top of ELO GaN stripes, consistent with the local CL spectra of Fig. 3a.

The spatial variation in the InGaN QW energy can be caused by a spatial variation of the In composition, and/or QW thickness. As has been shown in the GaAs materials system, the relative interfacet migration length of group III adatoms increases in the sequence In>Ga>Al.[8,9] It is thus natural to expect that the In will also have a longer migration length for III-nitride materials. The migration length may be longer on the $(10\bar{1}1)$ plane which is the slow growth plane under our growth conditions. We infer that during the QW growth, In atoms have a tendency to migrate from the $(10\bar{1}1)$ plane to the top of the ELO GaN stripes. As a result, the In composition and/or the thickness of QW on the top of stripes is larger than that on the sidewall and stripe edge.

We performed a single-band effective mass calculation of the QW interband energy to examine the effects of possible large variations in the QW thickness. The calculations show that a variation of the QW thickness of 4 nm to 40 nm will induce at most a ~9 nm shift of the QW peak wavelength. This small shift cannot sufficiently explain the measured 28 nm shift of QW peak wavelength. Therefore, we conclude that an In migration-induced spatial variation of the In composition in the QW is mostly responsible for the 28 nm red shift of QW peak wavelength, even though we cannot eliminate the possibility of a thickness variation contributing to the shifts we observe.

Figure 4a–d shows a line scan analysis of the QW peak wavelength versus e-beam position for samples A–D, respectively. For each sample, the QW energies are lower on the top of the stripes. Since the growth conditions for each sample were different, we can expect that the spatial variation of the QW energy will also be different. Samples A (ELO GaN stripe along $<11\bar{2}0>$) and B (ELO GaN stripe along $<1\bar{1}00>$) were grown under nominally the same growth conditions. For sample A, the QW energy gradually increases from the top to the bottom of the pyramids. A striking difference in this behavior is observed for sample B. Both the tops and bottoms of the pyramids exhibit a decrease in the QW energy, as shown in Fig. 4b. The

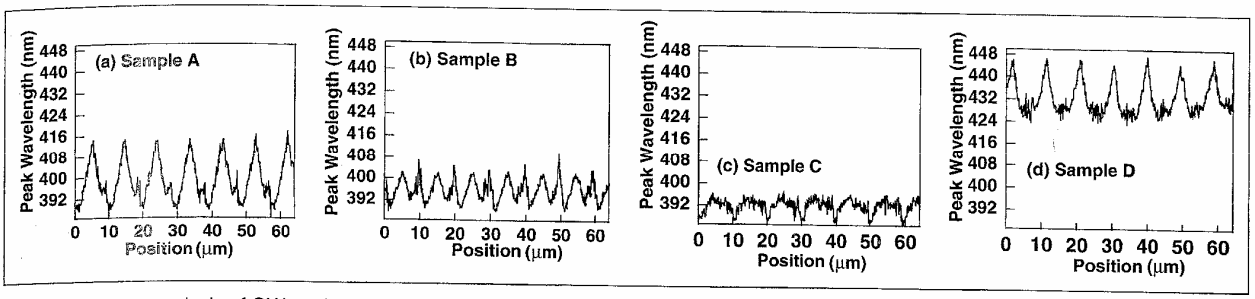

Fig. 4. Line scan analysis of QW peak wavelength for samples A, B, C, and D, respectively.

difference in side wall facets may lead to changes in the In migration length and path. By lowering the V/III ratio, the spatial variation in the In incorporation and resulting peak wavelength was considerably reduced, as shown in Fig. 4c. It is also likely that with a lower V/III ratio, a greater In desorption occurs during the QW growth, resulting in a reduced In migration along the facets and a reduced In incorporation into the QW. By increasing the QW growth temperature from 740°C to 775°C, as performed for the growth of sample D, the QW peak wavelength increased by 30 nm in comparison to that for sample A, as shown in Fig. 4d. The observance here is opposite to what one typically observed for InGaN QW grown on plane surface of (0001) plane. We tentatively attribute this to the QW growth on different planes [$(10\bar{1}1)$ plane vs. (0001) plane], which may have different growth mechanisms in certain temperature ranges.

The carrier relaxation kinetics were also studied by measuring time-delayed CL spectra for sample D at different time windows. The e-beam was rastered over an area of 64 μm × 47 μm, and the CL image of 440 nm is shown in Fig. 5a. The notation for the time-delayed spectra in Fig. 5b, D1–D5, denote time windows under which the spectra were acquired relative to the beginning of the decay of the luminescence. These time windows are referenced to the end of the electron beam pulses. The in-pulse window refers to a 3-ns wide acquisition window centered in the middle of the 50-ns wide e-beam pulse. During the decay stage of the luminescence, no shift of the main peak is detected in the D1–D5 windows. After 2.4 ns a broad peak around 400 nm appears, and reflects carriers which have been trapped in a higher bandgap region of the QW and which are unable to thermalize down to lower energy states. The origin of the peak is currently unclear. A previous study for InGaN/GaN QWs grown on the unpatterned surface of GaN (0001) showed a spectral diffusion and red shift of the main QW peak for increasing time windows.[10] The growth on pyramids in this study may limit the large In composition fluctuations previously attributed to the large time-dependent red-shifts.[10] Further underscoring this point, CL images of the InGaN QW grown on pyramid samples exhibit a much more homogeneous luminescence distribution in comparison to CL images of QWs grown on the unpatterned surface.[7,10] In the latter case, the strong carrier localization caused

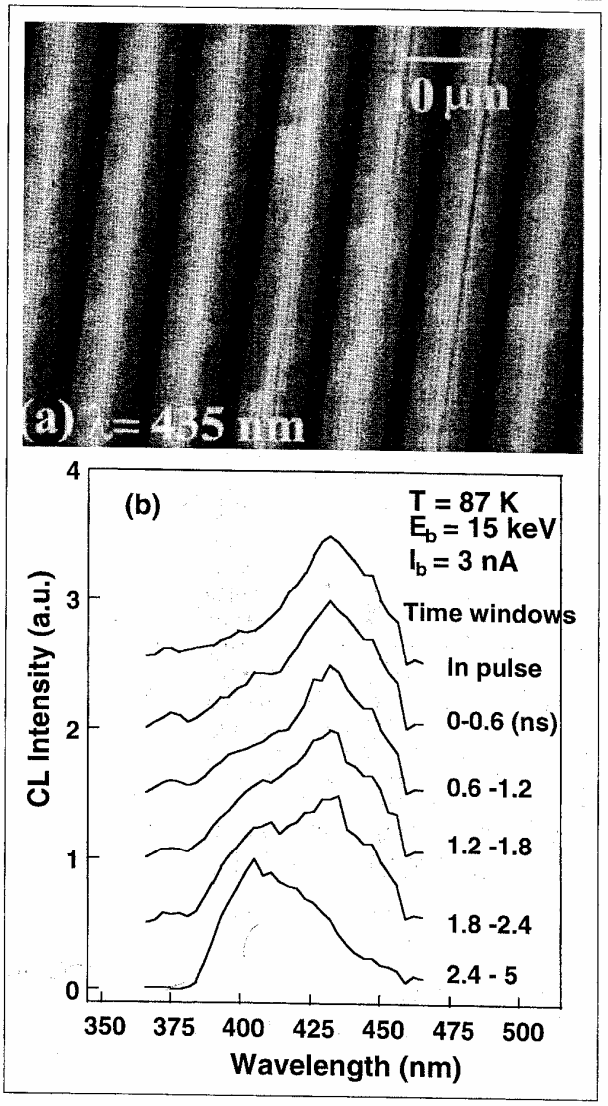

Fig. 5. (a) CL image, and (b) time-delayed CL spectra for sample D.

by InN-rich centers gave rise to large fluctuations in the spatial distribution of the luminescence. ELO GaN has a much lower density of dislocations relative to the GaN growth on planar samples.[1–4] Sugahara et al. have further shown that InGaN phase separation is affected by mixed dislocations.[11] Thus, we believe

that the relatively homogenous CL luminescence and apparently reduced phase separation for sample D is principally caused by the reduced density of dislocations in ELO GaN.

CONCLUSIONS

InGaN QWs grown on pyramids of ELO GaN were studied. Cathodoluminescence wavelength imaging, monochromatic CL imaging, and local CL spectroscopy show that In atoms have a tendency to migrate to the top of the ELO GaN stripe during growth. An increased migration and incorporation correlates with an increased red-shift of the InGaN QW energy. When the V/III ratio is reduced, the In incorporation as well as the migration to the top of ELO GaN stripes is also reduced. Increasing the QW growth temperature increases the In incorporation as shown by the red-shift of the QW peak wavelength. An investigation of the carrier relaxation by time-delayed CL spectra shows an absence of a large spectral diffusion in comparison to InGaN QWs grown on planar surfaces. These results suggest that composition fluctuations leading to spatially separated localized states are significantly reduced for growth on ELO samples. The successful growth of high-quality optically active InGaN QWs on patterned substrates further demonstrates progress in the eventual realization of new low dimensional III-nitride photonic devices.

ACKNOWLEDGEMENTS

This work was supported by DARPA through the UCSB GaN consortium and by ONR.

REFERENCES

1. A. Usui, H. Sunakawa, A. Sakai, and A. Yamaguchi, *Jpn. J. Appl. Phys.* 36, L899 (1997).
2. D. Kaplonek, S. Keller, R. Vetury, R.D. Underwood, P. Kozodoy, S.P. DenBaars, and U.K. Mishra, *Appl. Phys. Lett.* 71, 3569 (1997).
3. T.S. Zheleva, O.-H. Nam, M.D. Bremser, and R.F. Davis, *Appl. Phys. Lett.* 71, 2472 (1997).
4. N.P. Kobayashi, J.T. Kobayashi, X. Zhang, P.D. Dapkus, and D.H. Rich, *Appl. Phys. Lett.* 74, 2836 (1999).
5. S. Nakamura, M. Senoh, S. Nagahama, H. Iwasa, T. Yamada, T. Matsushita, H. Kiyoku, Y. Sugimoto, T. Kozaki, H. Umemoto, M. Sano, and K. Chocho, *Appl. Phys. Lett.* 72, 211 (1998).
6. J.T. Kobayashi, N.P. Kobayashi, P.D. Dapkus, X. Zhang, D.H. Rich, *Mater. Res. Soc. Symp. Proc. 468* (Warrendale, PA: MRS, 1997), p. 187.
7. X. Zhang, D.H. Rich, J.T. Kobayashi, N.P. Kobayashi, and P.D. Dapkus, *Appl. Phys. Lett.* 73, 1430 (1998).
8. X.Q. Shen, M. Tanaka, and T. Nishinaga, *J. Cryst. Growth* 127, 932 (1993).
9. E. Kapon, D.M. Hwang, M. Walther, R. Bhat, and N.G. Stoffel, *Surf. Sci.* 267, 593 (1992).
10. X. Zhang, D.H. Rich, J.T. Kobayashi, N.P. Kobayashi, and P.D. Dapkus, *Mat. Res. Soc. Symp. Proc. 512* (Warrendale, PA: MRS, 1998), p. 193.
11. T. Sugahara, M. Hao, T. Wang, D. Nakagawa, Y. Naoi, K. Nishino, and S. Sakai, *Jpn. J. Appl. Phys.*, Part 2, 37, L1195 (1998).